Multifunctional Dynamic Voltage Restorer Implementation with Resonance Controller for Emergency Control in Distribution Systems

[1] **V.S.V.S Pravallika,** [2] **T.Lakshminarayana**

M.Tech Student, KITS College of Engineering- Divili

Asst.Professor, KITS College of Engineering- Divili

Abstract - The dynamic voltage restorer(DVR) is a multifunction device used in distribution system to control voltage disturbances. In this paper , a multifunctional DVR protects the load voltage by posi-cast and P+ Resonant controllers when the source of disturbance is the parallel feeders. This posi-cast and P+ Resonance controllers improve the transient response and eliminate the steady state error in DVR response, respectively. The DVR acts as a virtual impedance with the main aim of protecting the Point of common coupling (PCC) voltage during downstream fault . The proposed algorithm is applied to some disturbances in load voltage caused by induction motors starting, and a three-phase short circuit fault. Also, the capability of the proposed DVR has been tested to limit the downstream fault current. Simulation results show the performance of the DVR to control the emergency conditions of the distribution systems.

Keywords **- Dynamic voltage restorer (DVR), emergency con-trol, voltage sag, voltage swell.**

1. Introduction

Voltage sag and voltage swell are two of the most impor-tant power-quality (PQ) problems that encompass almost 80% of the distribution system PQ problems [1]. According to the IEEE 1959–1995 standard, voltage sag is the decrease of 0.1 to 0.9 p.u. in the rms voltage level at system frequency and with the duration of half a cycle to 1 min [2]. Short circuits, starting large motors, sudden changes of load, and energization of trans-formers are the main causes of voltage sags [3].

According to the definition and nature of voltage sag, it can be found that this is a transient phenomenon whose causes are classified as low- or medium-frequency transient events [2]. In recent years, considering the use of sensitive devices in modern industries, different methods of compensation of voltage sags have been used. One of these methods is using

the DVR to im-prove the PQ and compensate the load voltage [6]–[13].

Previous works have been done on different aspects of DVR performance, and different control strategies have been found. These methods mostly depend on the purpose of using DVR. In some methods, the main purpose is to detect and compensate for the voltage sag with minimum DVR active power injection [4], [5]. Also, the in-phase compensation method can be used for sag and swell mitigation [6]. The multiline DVR can be used for eliminating the battery in the DVR structure and control-ling more than one line [7], [14]. Moreover, research has been made on using the DVR in medium level voltage [8]. Harmonic mitigation [9] and control of DVR under frequency variations [10] are also in the area of research. The closed-loop control with load voltage and current feedback is introduced as a simple method to control the DVR in [15]. Also, Posicast and P+Res-onant controllers can be used to improve the transient response and eliminate the steady-state error in DVR. The Posicast con-troller is a kind of step function with two parts and is used to improve the damping of the transient oscillations initiated at the start instant from the voltage sag. The P+Resonant con-troller consists of a proportional function plus a resonant func-tion and it eliminates the steady-state voltage tracking error [16]. The state feedforward and feedback methods [17], symmetrical components estimation [18], robust control [19], and wavelet transform [20] have also been proposed as different methods of controlling the DVR.

In all of the aforementioned methods, the source of distur-bance is assumed to be on the feeder which is parallel to the DVR feeder. In this paper, a multifunctional control system is proposed in which the DVR protects the load voltage using Posi-cast and P+Resonant controllers when the source of

disturbance is the parallel feeders. On the other hand, during a downstream fault, the equipment protects the PCC voltage, limits the fault current, and protects itself from large fault current. Although this latest condition has been described in [11] using the flux control method, the DVR proposed there acts like a virtual in-ductance with a constant value so that it does not receive any active power during limiting the fault current. But in the pro-posed method when the fault current passes through the DVR, it acts like a series variable impedance (unlike [11] where the equivalent impedance was a constant).

The basis of the proposed control strategy in this paper is that when the fault current does not pass through the DVR, an outer feedback loop of the load voltage with an inner feedback loop of the filter capacitor current will be used. Also, a feedforward loop will be used to improve the dynamic response of the load voltage. Moreover, to improve the transient response, the Posi-cast controller and to eliminate the steady-state error, the P+Res-onant controller are used. But in case the fault current passes through the DVR, using the flux control algorithm [11], the se-ries voltage is injected in the opposite direction and, therefore, the DVR acts like a series variable impedance.

The remainder of this paper is organized as follows: The general operation of DVR and its state space description are provided in Section II. The closed-loop control using Posicast and P+Res-onant controllers has been presented in Section III. In Section IV, the multifunctional DVR is introduced. The basis of the proposed control method is described in Section V. Finally, the simulation results are provided in Section VI which show that the control capability of the proposed DVR system is satisfactory.
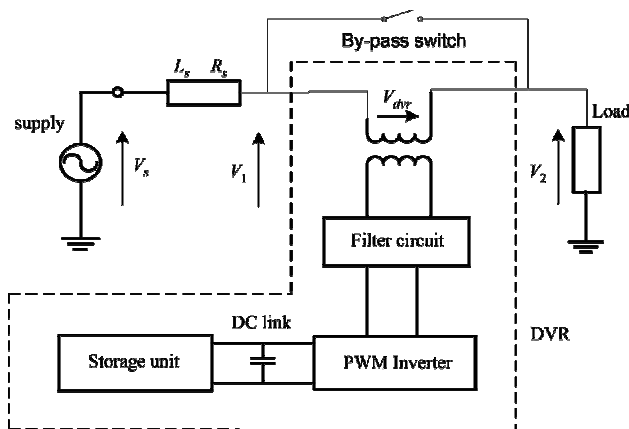
2. DVR Components and Its Basic Operational Principle

A. DVR Components

A typical DVR-connected distribution system is shown in Fig. 1, where the DVR consists of essentially a series-connected injection transformer, a voltage-source inverter, an inverter output filter, and an energy storage device that is connected to the dc link. Before injecting the inverter output to the system, it must be filtered so that harmonics due to switching function in the inverter are eliminated. It should be noted that when using the DVR in real situations, the injection transformer will be connected in parallel with a bypass switch (Fig. 1). When there is no disturbances in voltage, the injection transformer (hence, the DVR) will be short circuited by this switch to minimize losses and maximize cost effectiveness. Also, this switch can be in the form of two parallel thyristors, as they have high on and off speed [21]. A financial assessment of voltage sag events and use of flexible ac transmission systems (FACTS) devices, such as DVR, to mitigate them is provided in [22]. It is obvious that the flexibility of the DVR output depends on the switching accuracy of the pulsewidth modulation (PWM) scheme and the control method. The PWM generates sinusoidal signals by comparing a sinusoidal wave with a sawtooth wave and sending appropriate signals to the inverter switches. A further detailed description about this scheme can be found in [23].

B. Basic Operational Principle of DVR

The DVR system shown in Fig. 1, controls the load voltage by injecting an appropriate voltage phasor (V_{dvr}) in series with the
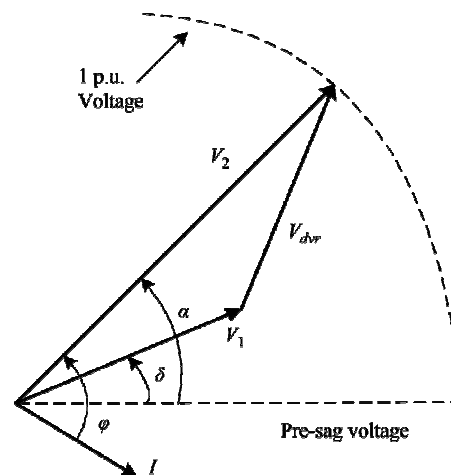

Fig. 1. Typical DVR-connected distribution system.

Fig. 2. Phasor diagram of the electrical conditions during a voltage sag.

IJCAT - International Journal of Computing and Technology, Volume 3, Issue 1, January 2016
ISSN : 2348 - 6090
www.IJCAT.org

system using the injection series transformer. In most of the sag compensation techniques, it is necessary that during compensa-tion, the DVR injects some active power to the system. There-fore, the capacity of the storage unit can be a limiting factor in compensation, especially during long-term voltage sags.

The phasor diagram in Fig. 2, shows the electrical conditions during voltage sag, where, for clarity, only one phase is shown. Voltages V_1, V_2, and V_{dvr} are the source-side voltage, the load-side voltage, and the DVR injected voltage, respectively. Also, the operators I, ϕ, δ, and α are the load current, the load power factor angle, the source phase voltage angle, and the voltage phase advance angle, respectively [24]. It should be noted that in addition to the in-phase injection technique, another technique, namely "the phase advance voltage compensation technique" is also used [24]. One of the advantages of this method over the in-phase method is that less active power should be transferred from the storage unit to the distribution system. This results in compensation for deeper sags or sags with longer durations.

Due to the existence of semiconductor switches in the DVR inverter, this piece of equipment is nonlinear. However, the state equations can be linearized using linearization techniques. The dynamic characteristic of the DVR is influenced by the filter and the load. Although the modeling of the filter (that usually is a simple LC circuit) is easy to do, the load modeling is not as simple because the load can vary from a linear time invariant one to a nonlinear time-variant one. In this paper, the simulations are performed with two types of loads: 1) a constant power load and 2) a motor load.

As Fig. 3 shows, the load voltage is regulated by the DVR through injecting V_{dvr}. For simplicity, the bypass switch shown in Fig. 1 is not presented in this figure. Here, it is assumed that the load has a resistance R_l and an inductance L_l. The DVR harmonic filter has an inductance of L_f, a resistance of R_f, and a capacitance of C_f. Also, the DVR injection transformer has a combined winding resistance of R_t, a leakage inductance of L_t, and turns ratio of $1:n$.

The Posicast controller is used in order to improve the tran-sient response. Fig. 4 shows a typical control block diagram of the DVR. Note that because in real situations, we are dealing with multiple feeders connected to a common bus, namely "the
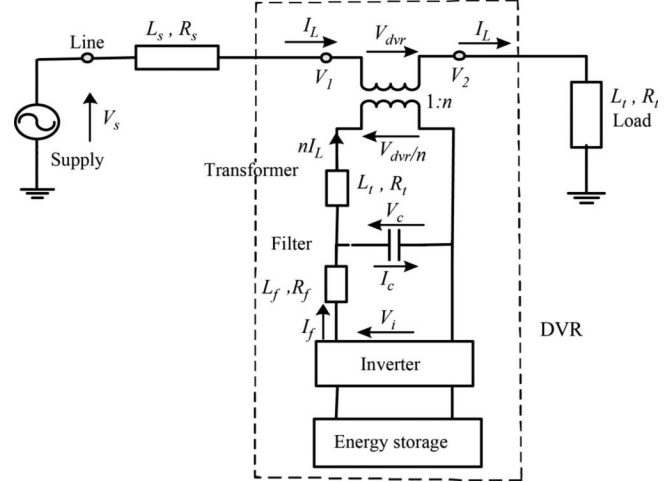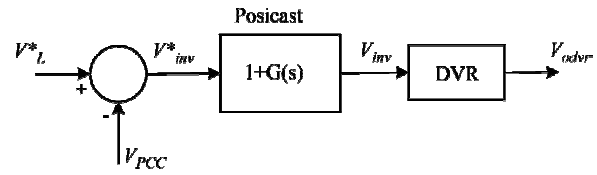

Fig. 3. Distribution system with the DVR.

Fig. 4. Open-loop control using the Posicast controller.

Point of Common Coupling (PCC)," from now on, V_1 and V_2 will be replaced with V_{PCC} and V_L, respectively, to make a gen-eralized sense. As shown in the figure, in the open-loop control, the voltage on the source side of the DVR (V_{PCC}) is compared with a load-side reference voltage (V_*) so that the necessary in-jection voltage V_{inv} is derived. A simple method to continue is to feed the error signal into the PWM inverter of the DVR. But the problem with this is that the transient oscillations initiated at the start instant from the voltage sag could not be damped suf-ficiently. To improve the damping, as shown in Fig. 4, the Posi-cast controller can be used just before transferring the signal to the PWM inverter of the DVR. The transfer function of the con-troller can be described as follows:

$$1 + G(s) = 1 + \frac{\delta}{1+\delta}\left(e^{-s^{T_d/2}} - 1\right)$$

(1)

where δ and T_d are the step response overshoot and the period of damped response signal, respectively. It should be noted that the Posicast controller has limited high-frequency gain; hence, low sensitivity to noise.

To find the appropriate values of δ and T_d, first the DVR model will be derived according to Fig. 3, as follows:

IJCAT - International Journal of Computing and Technology, Volume 3, Issue 1, January 2016
ISSN : 2348 - 6090
www.IJCAT.org

$$V_i = V_c + I_f R_f + L_f \frac{dI_f}{dt}$$
$$I_f = I_c + n \cdot I_l$$
$$I_c = C_f \frac{dV_c}{dt}$$
$$V_{dvr} = n \left[V_c - n \left(R_t I_t + L_t \frac{dI_t}{dt} \right) \right]$$
$$V_2 = V_1 + V_{dvr}. \qquad (2)$$

Then, according to (2) and the definitions of damping and the delay time in the control literature, δ and T_d are derived as follows:

$$T_d = \frac{2\pi}{\omega_r} = \frac{\pi}{\sqrt{\frac{1}{L_f C_f} - \frac{R_f^2}{4 L_f^2}}}$$
$$\delta = e^{\xi \pi / \sqrt{1 - \xi^2}} = e^{-R_f \pi \sqrt{C_f} / \sqrt{4 L_f - R_f^2 C_f}}. \qquad (3)$$

The Posicast controller works by pole elimination, and proper regulation of its parameters is necessary. For this reason, it is sensitive to inaccurate information of the system damping res-onance frequency. To decrease this sensitivity, as is shown in Fig. 5, the open-loop controller can be converted to a closed-loop controller by adding a multiloop feedback path parallel to the existing feedforward path. Inclusion of a feedforward and a feedback path is commonly referred to as two-degrees-of-freedom (2-DOF) control in the literature. As the name im-plies, 2-DOF control provides a DOF for ensuring fast dynamic tracking through the feedforward path and a second degree of freedom for the independent tuning of the system disturbance compensation through the feedback path [12]. The feedback path consists of an outer voltage loop and a fast inner current loop. To eliminate the steady-state voltage tracking error $(V_* - V_L)$, a computationally less intensive P+Resonant compensator is added to the outer voltage loop. The ideal P+Resonant com-pensator can be mathematically expressed as

$$G_R(s) = k_p + \frac{2 k_I s}{S^2 + \omega_0^2} \qquad (4)$$

where k_P and k_I are gain constants and $\omega_0 = 2\pi \times 50 \, rad / sec$ is the controller resonant frequency. Theoretically, the resonant controller compensates by introducing an infinite gain at the resonant frequency of 50 Hz (Fig. 6) to force the steady-state voltage error to zero. The ideal resonant controller, however, acts like a network with an infinite

quality factor, which is not realizable in practice. A more practical (nonideal) compensator is therefore used here, and is expressed as

$$G_R(s) = k_p + \frac{2 k_I \omega_{cut} S}{S^2 + 2\omega_{cut} S + \omega_0^2} \qquad (5)$$

where ω_{cut} is the compensator cutoff frequency which is 1 rad/s in this application [12].

Plotting the frequency response of (5), as in Fig. 6, it is noted that the resonant peak now has a finite gain of 40 dB which is sat-isfactorily high for eliminating the voltage tracking error [12]. In addition, a wider bandwidth is observed around the resonant frequency, which minimizes the sensitivity of the compensator to slight utility frequency variations. At other harmonic frequen-cies, the response of the nonideal controller is comparable to that of the ideal one.

3. Proposed Multifunctional DVR

In addition to the aforementioned capabilities of DVR, it can be used in the medium-voltage level (as in Fig. 7) to protect a group of consumers when the cause of disturbance is in the
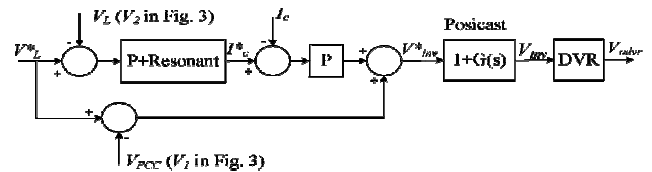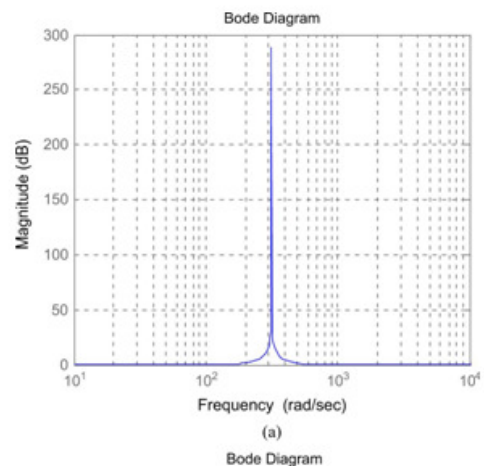

Fig. 5. Multiloop control using the Posicast and P+Resonant controllers.
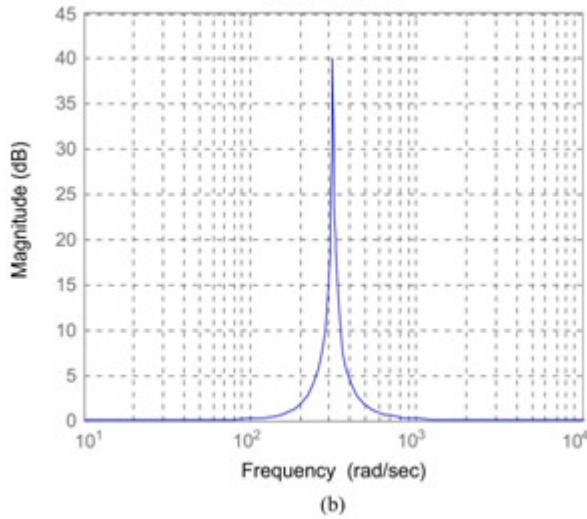

Fig. 6. (a) Bode Diagram

Fig. 6. Typical magnitude responses of the (a) Ideal and (b) nonideal P+Reso-nant controller.

downstream of the DVR's feeder and the large fault current passes through the DVR itself. In this case, the equipment can limit the fault current and protect the loads in parallel feeders until the breaker works and disconnects the faulted feeder.

The large fault current will cause the PCC voltage to drop and the loads on the other feeders connected to this bus will be affected. Furthermore, if not controlled properly, the DVR might also contribute to this PCC voltage sag in the process of compensating the missing voltage, hence further worsening the fault situation [11].
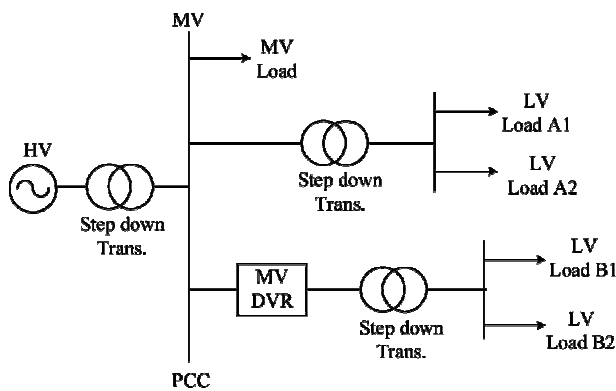
To limit the fault current, a flux-charge model has been pro-posed and used to make DVR act like a pure virtual induc-tance which does not take any real power from the external system and, therefore, protects the dc-link capacitor and bat-tery as shown in Fig. 1 [11]. But in this model, the value of the virtual inductance of DVR is a fixed one and the reference of the control loop is the flux of the injection transformer winding, and the PCC voltage is not mentioned in the control loop. In this paper, the PCC voltage is used as the main reference signal and the DVR acts like a variable impedance. For this reason, the absorption of real power is harmful for the battery and dc-link capacitor. To solve this problem, an impedance including a re-sistance and an inductance will be connected in parallel with the dc-link capacitor. This capacitor will be separated from the cir-cuit, and the battery will be connected in series with a diode just when the downstream fault occurs so that the power does not enter the battery and the dc-link capacitor. It should be noted here that the inductance is used mainly to prevent large oscilla-tions in the current. The active power mentioned is, therefore, absorbed by the impedance.

4. Proposed Method for Using The Flux-Charge Model

In this part, an algorithm is proposed for the DVR to restore the PCC voltage, limit the fault current, and, therefore, protect the DVR components. The flux-charge model here is used in a way so that the DVR acts as a virtual inductance with a variable value in series with the distribution feeder. To do this, the DVR must be controlled in a way to inject a proper voltage having the
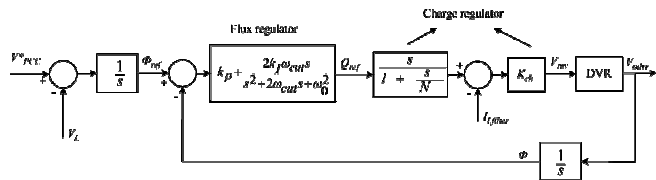
Fig. 8. Proposed method.

opposite polarity with respect to usual cases. It should be noted that overcurrent tripping is not possible in this case, unless ad-ditional communication between the DVR and the downstream side overcurrent circuit breaker (CB) is available. If it is neces-sary to operate the overcurrent CB at PCC, communication be-tween the DVR and the PCC breaker might have to be made and this can be easily done by sending a signal to the breaker when the DVR is in the fault-current limiting mode as the DVR is just located after PCC [11]. The proposed DVR control method is illustrated in Fig. 8. It should also be noted that the reference flux $\left(\Phi_{ref} \right)$ is derived by integration of the subtraction of the PCC reference

Fig. 7. DVR connected in a medium-voltage level power system.

voltage (V_*) and the DVR load-side voltage. In this control strategy, the control variable used for the outer flux model is the inverter-filtered terminal flux defined as:

$$\Phi = \int V_{\mathrm{odvr}} \mathrm{dt}$$

(6)

where V_{odvr} is the filter capacitor voltage of the DVR (at the DVR power converter side of the injection transformer). The flux error is then fed to the flux regulator, which is a P+Resonant controller, with a transfer function given in (6). On the other hand, it can be shown that a single flux-model would not damp out the resonant peak of the LC filter connected to the output of the inverter.

To stabilize the system, an inner charge model is therefore considered. In this loop, the filter inductor charge, which is de-rived by integration of its current, tracks the reference charge output Q_{ref} of the flux regulator. The calculated charge error is then fed to the charge regulator with the transfer function

$$G_{\mathrm{charge}}(s) = k_{Ch} \frac{S}{1 + \frac{S}{N}}$$
(7)

which is actually a practical form of the derivative controller. In this transfer function, the regulator gain is limited to N at high frequencies to prevent noise amplification.

The derivative term in $S/1 + S/N$ neutralizes the effects of voltage and current integrations at the inputs of the flux-charge model, resulting in the proposed algorithm having the same regulation performance as the multiloop voltage-current feed-back control, with the only difference being the presence of an additional low–pass filter in the flux control loop in the form of $1/1 + S/N$. The bandwidth of this low–pass filter is tuned (through varying N) with consideration for measurement noise attenuation, DVR LC-filter transient resonance attenuation, and system stability margins.

Fig. 9. Under study test system.

V. SIMULATION RESULTS

In this part, the proposed DVR topology and control algorithm will be used for emergency control during the voltage sag. The three-phase short circuit and the start of a three-phase large induction motor will be considered as the cause of distortion in the simulations.

A. Under Study Test System

In this paper, the IEEE standard 13-bus balanced industrial system will be used as the test system. The one-line diagram of this system is shown in Fig. 9.

The test system is modeled in PSCAD/EMTDC software. Control methods of Figs. 5 and 8 were applied to control the DVR, and the voltage, current, flux, and charge errors were included as the figures show. Also, the DVR was modeled by its components (instead of its transfer functions) in the PSCAD/EMTDC software to make more real simulation re-sults. A 12-pulse inverter was used so that each phase could be controlled separately. Detailed specifications of the DVR components are provided in the Appendix.

The plant is fed from a utility supply at 69 kV and the local plant distribution system operates at 13.8 kV. The local (in-plant) generator is represented as a simple Thevenin equiv-alent. The internal voltage, determined from the converged power-flow solution, is $13.8\angle\_1.52\circ$ kV.

The equivalent impedance is the subtransient impedance which is $0.0366 + j\angle1.3651\,\Omega$. The plant power factor cor-rection capacitors are rated at 6000 kvar. As is typically done,

IJCAT - International Journal of Computing and Technology, Volume 3, Issue 1, January 2016
ISSN : 2348 - 6090
www.IJCAT.org

leakage and series resistance of the bank are neglected in this study. The detailed description of the system can be found in [25]. In the simulations, the DVR is placed between buses "03:MILL-1" and "05:FDR F."

B. Three-Phase Short Circuit

In this part, the three-phase short circuit is applied on bus "26:FDR G," and the capability of the DVR in protecting the voltage on bus "05:FDR F" will be studied. The DVR param-eters and the control system specifications are provided in Ap-pendices A and B. At $t= 205$ ms, the fault is applied at $t= 285$ ms, and the breaker works and separates the line between buses "03:MILL-1" and "26:FDR G" from the system. At $t= 305$ ms, the fault will be recovered and, finally, at $t= 310$ ms, the separated line will be rejoined to the system by the breaker. The simulation results are shown in Fig. 10.

As can be seen in the figure, the rms voltage of PCC drops to about 0.25 p.u. during the fault. It is obvious that this remaining voltage is due to the impedances in the system. The DVR will start the compensation just after the detection of sag. As can be seen in the enlarged figure, the DVR has restored the voltage to normal form with attenuation of the oscillations at the start of the compensation in less than half a cycle. It is worth noting that the amount and shape of the oscillations depends also on the time of applying the fault. As can be seen in the enlarged figure, the voltage value of phase B is nearly zero; this phase has minimum oscillation when the fault starts.

C. Starting the Induction Motor

A large induction motor is started on bus "03:MILL-1." The motor specifications are provided in Appendix C. The large motor starting current will cause the PCC voltage (bus "03:MILL-1" voltage) to drop. The simulation results in the case of using the DVR are shown in Fig. 11. In this simulation, the motor is started at $t= 405$ ms. As can be seen in Fig. 11, at this time, the PCC rms voltage drops to about 0.8 p.u. The motor speed reaches the nominal value in about 1 s. During this period, the PCC bus is under voltage sag. From $t= 1.4$ s, as the speed approaches nominal, the voltage also approaches the normal condition. However, during all of these events, the DVR keeps the load bus voltage (bus "05:FDR F" voltage) at the normal condition. Also, as can be seen in the enlarged version of Fig. 11, the DVR has succeeded in restoring the load voltage in half a cycle from the instant of the motor starting.

D. Fault Current Limiting

The last simulation is run for a symmetrical downstream fault, and the capability of the DVR to reduce the fault

current and restore the PCC voltage is tested. For this purpose, a three-phase short circuit is applied on bus "05:FDR F". In Fig. 12, the fault current, without the DVR compensation, is shown. For the simulation with DVR compensation, the three-phase fault is applied at $t= 205$ ms and then removed after 0.1 s. Also, a breaker will remove the faulted bus from the entire system at $t= 300$ ms. Fig. 13 shows the DVR operation during the fault.

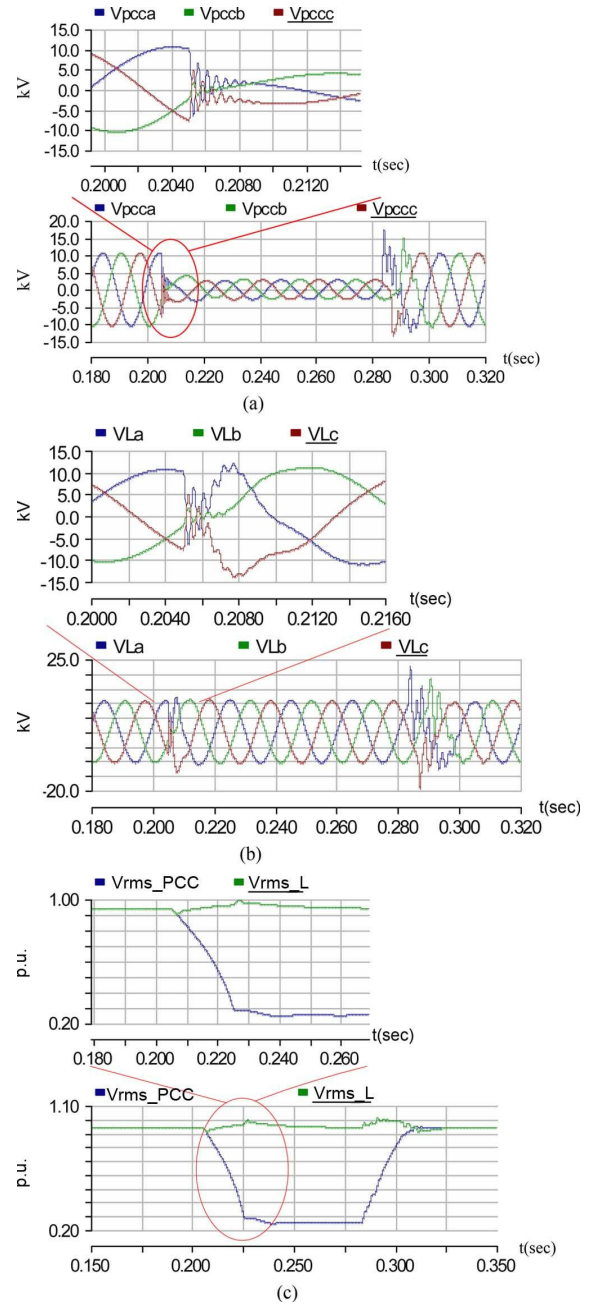As can be seen, the rms load bus voltage reaches zero during the

Fig. 10. Three-phase fault compensation by DVR. (a) Three-phase PCC volt-ages. (b) Three-phase load voltages. (c) RMS voltages of PCC and load.

fault, and as the enlarged figure shows, in about half a cycle, the DVR has succeeded in restoring the PCC voltage waveshape to the normal condition. It should be noted that the amount and shape of the oscillations depend on the time of applying the fault. As Fig. 13 shows, at this time, the voltage value of phase B is nearly zero; this phase has the minimum oscillation when the fault starts. Also, the maximum value of the fault current has been reduced from 40 kA (see Fig. 12) to 5 kA with DVR compensation.

Fig. 12. Current waveshape due to the three-phase short-circuit fault without DVR compensation.

Fig. 11. Starting of an induction motor and the DVR compensation. (a) Three-phase PCC voltages. (b) Three-phase load voltages. (c) RMS voltages of PCC and load.
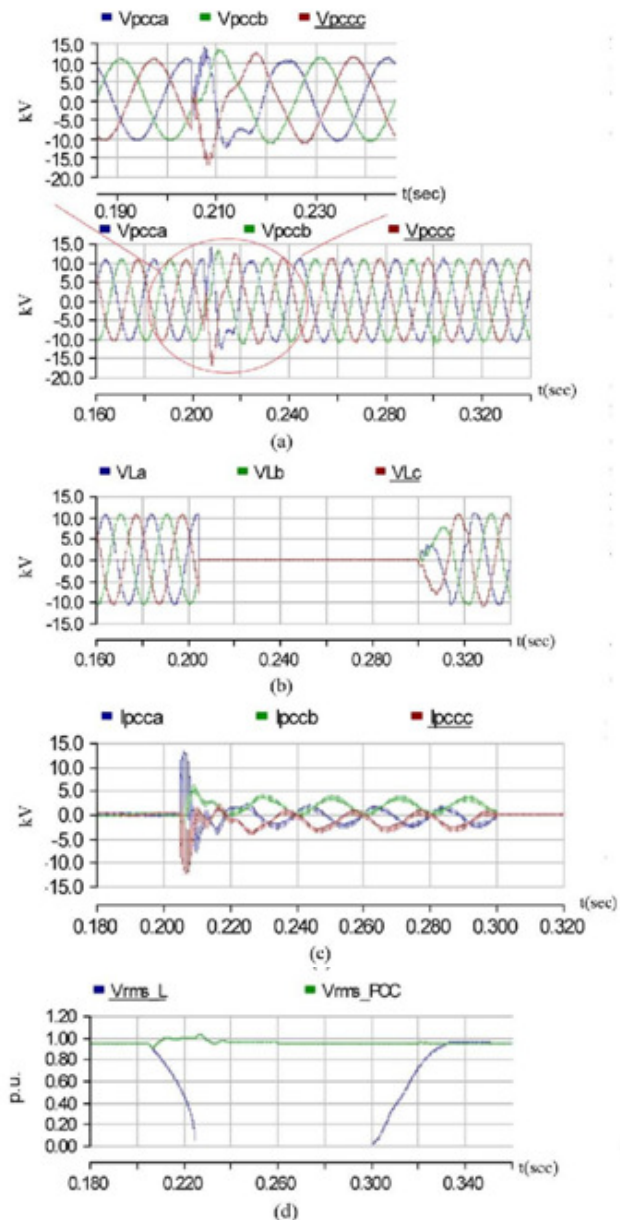

Fig. 13. Fault current limiting by DVR. (a) Three-phase PCC voltages. (b) Three-phase load voltages. (c) Three-phase currents. (d) RMS voltages of the PCC and load.

has been reduced from 40 kA (see Fig. 12) to 5 kA with DVR compensation.

VI. CONCLUSION

In this paper, a multifunctional DVR is proposed, and a closed-loop control system is used for its control to improve the damping of the DVR response. Also, for further improving the transient response and eliminating the steady-state error, the Posicast and P+Resonant controllers are used. As the second function of this DVR, using the flux-charge model, the equipment is controlled so that it limits the downstream fault currents and protects the PCC voltage during these faults by
acting as a variable impedance. The problem of absorbed active power is solved by entering an impedance just at the start of this kind of fault in parallel with the dc-link capacitor and the battery being connected in series with a diode so that the power does not enter it. The simulation results verify the effectiveness and capability of the proposed DVR in compensating for the voltage sags caused by short circuits and the large induction motor starting and limiting the downstream fault currents and protecting the PCC voltage.

APPENDIX

DVR Parameters:
Filter inductance $(Lf) = 1$ mH
Filter capacitance $(Cf) = 700 \mu$F
Inverter modulation ratio=21 mF
Kind of DVR inverter: 12 Pulse
DC-link capacitance: 26 mF
Entered resistance for current limiting: 3 ohms
Entered inductance for current limiting: 2 mH
Supply battery: 12 kV.
Control System Parameters:
$\delta = 1$
$T_d = 41.56 \mu$s
$K_p = 1$
$K_I = 100$
$\omega_0 = 314$ rad/s
$\omega_{cut} = 1.0$ rad/s.
Induction Motor Parameters:
Rated power: 2.4 MVA
Rated voltage: 13.8 kV
Moment of inertia: 3.7267 sec
Number of rotor squirrel cages: 1
Base frequency: 50 Hz
Stator resistance: 0.0034 p.u.
Rotor resistance: 0.298 p.u
Stator inductance: 0.0102 p.u.
Rotor inductance: 0.05 p.u
Magnetizing inductance: 0.9 p.u.

References

[1] J. A. Martinez and J. Martin-Arnedo, "Voltage sag studies in distri-bution networks- part II: Voltage sag assessment," *IEEE Trans. Power Del.*, vol. 21, no. 3, pp. 1679–1688, Jul. 2006.

[2] J. A. Martinez and J. M. Arnedo, "Voltage sag studies in distribution networks- part I: System modeling," *IEEE Trans. Power Del.*, vol. 21, no. 3, pp. 338–345, Jul. 2006.

[3] P. Hcine and M. Khronen, "Voltage sag distribution caused by power system faults," *IEEE Trans. Power Syst.*, vol. 18, no. 4, pp. 1367–1373, Nov. 2003.

[4] S. S. Choi, B. H. Li, and D. M. Vilathgamuwa, "Dynamic voltage restoration with minimum energy injection," *IEEE Trans. Power Syst.*, vol. 15, no. 1, pp. 51–57, Feb. 2000.

[5] C. Fitzer, M. Barnes, and P. Green, "Voltage sag detection technique for a dynamic voltage restore," *IEEE Trans. Ind. Appl.*, vol. 2, no. 1, pp. 203–212, Jan./Feb. 2004.

[6] C. Benachaiba and B. Ferdi, "Voltage quality improvement using DVR," *Electt. Power Qual. Utilisation, Journal*, vol. XIV, no. 1, 2008.

[7] D. M. Vilathgamuwa, H. M. Wijekoon, and S. S. Choi, "A novel tech-nique to compensate voltage sags in multiline distribution system-the interline dynamic voltage restorer," *IEEE Trans. Ind. Electron.*, vol. 53, no. 5, pp. 1603–1611, Oct. 2006.

[8] J. G. Nielsen, M. Newman, H. Nielsen, and F. Blaabjerg, "Control and testing of a dynamic voltage restorer (DVR) at medium voltage level," *IEEE Trans. Power Electron.*, vol. 19, no. 3, pp. 806–813, May 2004.

[9] M. J. Newman, D. G. Holmes, J. G. Nielsen, and F. Blaabjerg, "A dy-namic voltage restorer (DVR) with selective harmonic compensation at medium voltage level," *IEEE Trans. Ind. Appl.*, vol. 41, no. 6, pp. 1744–1753, Nov./Dec. 2005.

[10] A. K. Jindal, A. Ghosh, and A. Joshi, "Critical load bus voltage control using DVR under system frequency variation," *Elect. Power Syst. Res.*, vol. 78, no. 2, pp. 255–263, Feb. 2008.

[11] Y. W. Li, D. M. Vilathgamuwa, P. C. Loh, and F. Blaabjerg, "A dual-functional medium voltage level DVR to limit downstream fault cur-rents," *IEEE Trans. Power Electron.*, vol. 22, no. 4, pp. 1330–1340, Jul. 2007.

[12] P. C. Loh, D. M. Vilathgamuwa, S. K. Tang, and H. L. Long, "Multi-level dynamic voltage restorer," *IEEE Power Electron. Lett.*, vol. 2, no. 4, pp. 125–130, Dec. 2004.

[13] E. Babaei, M. Farhadi, and M. Sabahi, "Compensation of voltage dis-turbances in distribution systems using single-phase dynamic voltage restorer," *Elect. Power Syst. Res.*, Jul. 2010.

[14] C. N.-M. Ho and H. S.-H. Chung, "Implementation and performance evaluation of a fast dynamic control scheme for capacitor-supported interline DVR," *IEEE Trans Power Electron.*, vol. 25, no. 8, pp. 1975–1988, Aug. 2010.

[15] M. Vilathgamuwa, A. A. D. R. Perera, and S. S. Choi, "Performance improvement of the dynamic voltage restorer with closed-loop load voltage and current-mode control," *IEEE Trans. Power Electron.*, vol. 17, no. 5, pp. 824–834, Sep. 2002.

[16] Y. W. Li, P. C. Loh, F. Blaabjerg, and D. M. Vilathgamuwa, "Investiga-tion and improvement of transient response of DVR at medium voltage level," *IEEE Trans. Ind. Appl.*, vol. 43, no. 5, pp. 1309–1319, Sep./Oct. 2007.

[17] H. Kim and S. K. Sul, "Compensation voltage control in dynamic voltage restorers by use of feedforward and state feedback scheme," *IEEE Trans. Power Electron.*, vol. 20, no. 5, pp. 1169–1177, Sep. 2005.

[18] M. I. Marei, E. F. El-Saadany, and M. M. A. Salama, "A new approach to control DVR based on symmetrical components estimation," *IEEE Trans. Power Del.*, vol. 22, no. 4, pp. 2017–2024, Oct. 2007.

[19] Y. W. Li, D. M. Vilathgamuwa, F. Blaabjerg, and P. C. Loh, "A robust control scheme for medium-voltage-level DVR implementation," *IEEE Trans. Ind. Electron.*, vol. 54, no. 4, pp. 2249–2261, Aug. 2007.

[20] S. A. Saleh, C. R. Moloney, and M. A. Rahman, "Implementation of a dynamic voltage restorer system based on discrete wavelet transforms," *IEEE Trans. Power Del.*, vol. 23, no. 4, pp. 2360–2375, Oct. 2008.

[21] H. Awad, J. Svensson, and M. Bollen, "Mitigation of unbalanced voltage dips using static series compensator," *IEEE Trans Power Electron.*, vol. 19, no. 3, pp. 837–846, May 2004.

[22] J. V. Milanovic and Y. Zhang, "Global minimization of financial losses due to voltage sags with FACTS based devices," *IEEE Trans. Power Del.*, vol. 25, no. 1, pp. 298–306, Jan. 2010.

[23] M. H. Rashid, *Power Electronics-Circuits, Devices and Applications*, 3rd ed. India: Prentice-Hall of India, Aug. 2006.

[24] M. Vilathgamua, A. A. D. R. Perara, S. S. Choi, and K. J. Tseng, "Control of energy optimized dynamic voltage restorer," in *Proc. IEEE IECON Conf.*, San Jose, CA, 1999, vol. 2, pp. 873–878.

[25] "Task force on harmonics modeling & simulation (co-author), test sys-tems for harmonics modeling and simulation," *IEEE Trans. Power Del.*, vol. 14, no. 2, pp. 579–585, Apr. 1999.